We are IntechOpen, the world's leading publisher of Open Access books Built by scientists, for scientists

4,800
Open access books available

122,000
International authors and editors

135M
Downloads

Our authors are among the

154
Countries delivered to

TOP 1%
most cited scientists

12.2%
Contributors from top 500 universities

CLARIVATE ANALYTICS BOOK CITATION INDEX INDEXED

WEB OF SCIENCE™

Selection of our books indexed in the Book Citation Index in Web of Science™ Core Collection (BKCI)

Interested in publishing with us?
Contact book.department@intechopen.com

Numbers displayed above are based on latest data collected.
For more information visit www.intechopen.com

12

Dynamics of Hexapods with Fixed-Length Legs

Rosario Sinatra[a] and Fengfeng Xi[b]
[a]*Università di Catania, 95125, Catania,*
[b]*Ryerson University Toronto, Ontario,*
[a]*Italy*
[b]*Canada*

1. Introduction

Hexapod is a new type of machine tool based on the parallel closed-chain kinematic structure. Compared to the conventional machine tool, parallel mechanism structure offers superior stiffness, lower mass and higher acceleration, resulting from the parallel structural arrangement of the motion systems. Moreover, hexapod has the potential to be highly modular and re-configurable, with other advantages including higher dexterity, simpler and fewer fixtures, and multi-mode manufacturing capabilities.

Initially, hexapod was developed based on the Stewart platform, i.e. the prismatic type of parallel mechanism with the variable leg length. Commercial hexapods, such as VARIAX from Giddings & Lewis, Tornado from Hexel Corp., and Geodetic from Geodetic Technology Ltd., are all based on this structure. One of the disadvantages for the variable leg length structure is that the leg stiffness varies as the leg moves in and out. To overcome this problem, recently the constant leg length hexapod has been envisioned, for instance, HexaM from Toyada (Susuki et al., 1997). Hexaglibe form the Swiss Federal Institute of Techonology (Honegger et al., 1997), and Linapod form University of Stuttgart (Pritschow & Wurst, 1997). Between these two types, the fixed-length leg is stiffer (Tlusty et al., 1999) and, here, becoming popular.

Dynamic modeling and analysis of the parallel mechanisms is an important part of hexapod design and control. Much work has been done in this area, resulting in a very rich literature (Fichter, 1986; Sugimoto, 1987; Do & Yang, 1988; Geng et al., 1992; Tsai, 2000; Hashimoto & Kimura, 1989; Fijany & Bejezy, 1991). However, the research work conducted so far on the inverse dynamics has been focused on the parallel mechanisms with extensible legs.

In this chapter, first, in the inverse dynamics of the new type six d.o.f. hexapods with fixed-length legs, shown in Fig. 1, is developed with consideration of the masses of the moving platform and the legs. (Xi & Sinatra, 2002) This system consists of a moving platform *MP* and six legs sliding along the guideways that are mounted on the support structure. Each leg is connected at one end to the guideway by a universal joint and at another end to the moving platform by a spherical joint. The natural orthogonal complement method (Angeles & Lee, 1988; Angeles & Lee, 1989) is applied, which provides an effective way of solving multi-body dynamics systems. This method has been applied to studying serial and parallel manipulators (Angeles & Ma, 1988; Zanganesh et al., 1997) automated vehicles (Saha & Angeles, 1991) and flexible mechanisms (Xi & Sinatra, 1997). In this development, the

Source: Parallel Manipulators, Towards New Applications, Book edited by: Huapeng Wu, ISBN 978-3-902613-40-0, pp. 506, April 2008, I-Tech Education and Publishing, Vienna, Austria

Newton-Euler formulation is used to model the dynamics of each individual body, including the moving platform and the legs. All individual dynamics equations are then assembled to form the global dynamics equations. Based on the complete kinematics model developed, an explicit expression is derived for the natural orthogonal complement which effectively eliminates the constraint forces in the global dynamics equations. This leads to the inverse dynamics equations of hexapods that can be used to compute required actuator forces for given motions.

Fig. 1. New hexapod design

Finally, for completeness of the dynamic study of the parallel manipulator with the fixed-length legs, the static balancing is studied (Xi et al., 2005).

A great deal of work has been carried out and reported in the literature for the static balancing problem. For example, in the case of serial manipulator, Nathan (Nathan, 1985) and Hervé (Hervé, 1986) applied the counterweight for gravity compensations. Streit et al. (Streit & Gilmore, 1991), (Walsh et al., 19) proposed an approach to static balanced rotary bodies and two degrees of freedom of the revolute links using springs. Streit and Shin presented a general approach for the static balancing of planar linkages using springs(Streit & Shin, 1980). Ulrich and Kumar presented a method of passive mechanical gravity compensation using appropriate pulley profiles (Ulrich & Kumar, 1991). Kazerooni and Kim presented a method for statically-balanced direct drive arm (Kazerooni & Kim, 1990).

For the parallel manipulator much work was done by Gosselin et al. Research reported in (Gosselin & Wang, 1998) was focused on the design of gravity-compensated of a six–degree-of-freedom parallel manipulator with revolute joints. Each leg with two links is connected by an actuated revolute joint to the base platform and by a spherical joints the moving platform. Two methods are used, one approach using the counterweight and the other using springs. In the former method, if the centre of mass of a mechanism can be made stationary, the static balancing is obtained in any direction of the Cartesian space. In the second approach, if the total energy is kept constant, the mechanism is statically balanced only in the direction of gravity vector. The static balancing conditions are derived for the three-degree-of-freedom spatial parallel manipulator (Wang & Gosselin, 1998) and in similar

conditions are obtained for spatial four-degree-of-freedom parallel manipulator using two common methods, namely, counterweights and springs (Wang & Gosselin, 2000).
In this chapter, following the same approach presented by Gosselin, the static balancing of the six d.o.f. platform type parallel manipulator with the fixed-length legs shown is studied. The mechanism can be balanced using the counterweight with a smart design of pantograph. The mechanism can be balanced using the method, i.e., the counterweight with a smart design of pantograph. By this design a constant global center of mass for any configurations of the manipulator is obtained.
Finally, the leg masses become important for hexapods operating at high speeds, such as high-speed machining; then in the future research and development the effect of leg inertia on hexapod dynamics considering high-speed applications will be investigated.

2. Kinematic modeling

2.1 Notation

As shown in Figure 2, this hexapod system consists of a moving platform *MP* to which a tool is attached, and six legs sliding along the guideways that are mounted on the support structure including the base platform *BP*. Each leg is connected at one end to the guideway by a universal joint and at another end to the moving platform by a spherical joint.

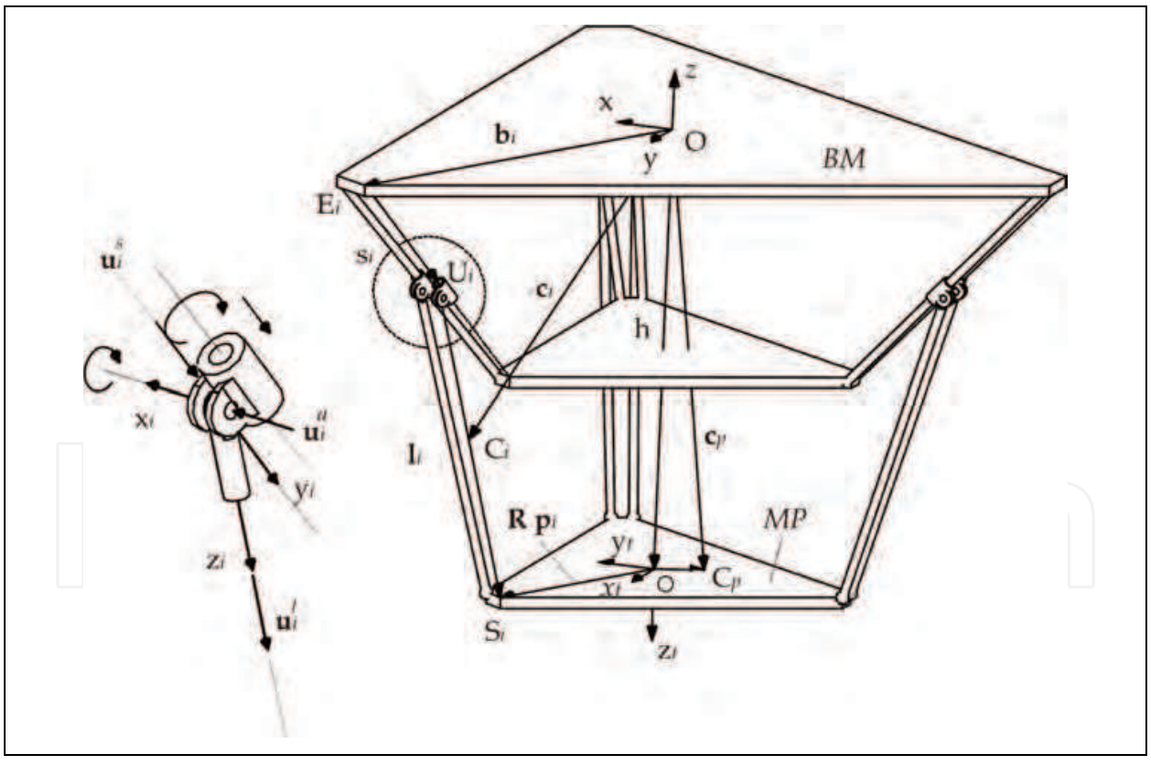

Fig. 2. Kinematic notation of the *i*th leg

The coordinate systems used are a fixed coordinate system O-xyz is attached to the base and a local coordinate system O_t-$x_ty_tz_t$ attached to the moving platform. Vector $\mathbf{b}_i$, $\mathbf{s}_i$, and $\mathbf{l}_i$ are directed from O to B_i, from B_i to U_i, and from U_i to S_i respectively. B_i indicates the position of one end of the *i*th guideway attached to the base, U_i indicates the position of the *i*th

universal joint, and S_i indicates the position of the ith spherical joint. Six legs are numbered from 1 to 6.

Furthermore, a local coordinate frame O_i-$x_iy_iz_i$ is defined for each leg, with its origin located at the center of the ith universal joint. Two unit vectors are used. Unit vector $\mathbf{u}_i^l$ is along the leg length representing the direction of the ith leg, and unit vector $\mathbf{u}_i^s$ is along the guideway representing the direction of the ith guideway. The orientation of the ith coordinate frame with respect to the base can therefore be defined by a 3×3 rotation matrix, for i = 1,…,6, as

$$\mathbf{Q}_i = \begin{bmatrix} \mathbf{u}_i^a & \mathbf{u}_i^l \times \mathbf{u}_i^a & \mathbf{u}_i^l \end{bmatrix} \tag{1}$$

where $\mathbf{u}_i^a$ is expressed as

$$\mathbf{u}_i^a = \frac{\mathbf{u}_i^s \times \mathbf{u}_i^l}{\left\| \mathbf{u}_i^s \times \mathbf{u}_i^l \right\|} \tag{2}$$

Note that vector $\mathbf{u}_i^l$ is configuration-dependent and determined for the given location of the moving platform; vector $\mathbf{u}_i^s$ is constant and defined by the geometry of the hexapod.

For the purpose of carrying out the inverse dynamics analysis of the hexapod, the following symbols are defined. As shown in Figure 2, C_i is the center of mass of the ith leg, C_p is the center of mass of the moving platform, $\mathbf{c}$, $\dot{\mathbf{c}}$ and $\ddot{\mathbf{c}}$ are the position, velocity and acceleration vectors, respectively, of C_i with respect to the fixed coordinate frame, $\bar{\boldsymbol{\rho}}$ is the vector pointing from O_t to C_p with respect to the local coordinate frame O_t-$x_ty_tz_t$.

2.2 Kinematics

Consider one branch of the leg-guideway system, as shown in Figure 2, the following loop equation for i = 1,…,6, holds,

$$\mathbf{h} + \mathbf{R}\bar{\mathbf{p}}_i - \mathbf{b}_i - \mathbf{s}_i - \mathbf{l}_i = \mathbf{0} \tag{3}$$

where $\mathbf{h}$ and $\mathbf{R}$ are the vector and rotation matrix that define the position and orientation of the moving platform relative to the base, respectively, $\bar{\mathbf{p}}_i$ is the vector representing the position of the ith spherical joint on the moving platform in the local coordinates.

Since the leg always moves along the guideway, $\mathbf{s}_i$ can be expressed as

$$\mathbf{s}_i = s_i \mathbf{u}_i^s \tag{4}$$

where s_i is a scalar representing the displacement of the ith actuator along the guideway. Likewise, leg vector $\mathbf{l}_i$ can be expressed as

$$\mathbf{l}_i = l_i \mathbf{u}_i^l \tag{5}$$

where l_i is a scalar representing the fixed length of the ith leg. As mentioned in Section 2.1, the leg axis is parallel to the z_i axis of the local coordinate frame O_i-$x_iy_iz_i$. In the light of eq.(1), $\mathbf{u}_i^l$ can be expressed as

$$\mathbf{u}_i^l = \mathbf{Q}_i \mathbf{z}_i \tag{6}$$

Substituting eqs.(4 & 5) into eq.(3) and rearranging it yields the following kinematics equations for the fixed-length leg hexapod, for i = 1,…,6,

$$s_i \mathbf{u}_i^s = \mathbf{h} + \mathbf{R}\bar{\mathbf{p}}_i - \mathbf{b}_i - l_i \mathbf{u}_i^l \tag{7}$$

To obtain the velocity of the moving platform, taking the time derivative of eq. (7) yields

$$\dot{s}_i \mathbf{u}_i^s = \mathbf{v} + (\boldsymbol{\omega} \times \mathbf{R}\bar{\mathbf{p}}_i) - (\boldsymbol{\omega}_i \times \mathbf{l}_i) \tag{8}$$

where $\mathbf{v}$ and $\boldsymbol{\omega}$ are the vectors representing the velocity and angular velocity of the moving platform, respectively, and $\boldsymbol{\omega}$ is the vector representing the angular velocity of the ith leg. Furthermore, by taking dot product on both sides of eq.(8) by $\mathbf{l}_i$, it leads to

$$\dot{s}_i \mathbf{u}_i^s \cdot \mathbf{l}_i = [\mathbf{v} + (\boldsymbol{\omega} \times \mathbf{R}\bar{\mathbf{p}}_i)] \cdot \mathbf{l}_i \tag{9}$$

It is well known that the kinematic analysis of parallel manipulator leads to two Jacobian matrices, namely, the forward and the inverse Jacobian (Gosselin & Angeles, 1990). To find the Jacobians for the hexapod under study, rearranging eq.(9) yields the following form

$$\dot{s}_i \left(\mathbf{u}_i^s \cdot \mathbf{l}_i \right) = [\mathbf{l}_i^T, (\mathbf{R}\bar{\mathbf{p}}_i \times \mathbf{l}_i)^T] \mathbf{t}_p \tag{10}$$

where $\mathbf{t} = \left[\mathbf{v}, \boldsymbol{\omega} \right]$ is the 6×1 twist vector of the moving platform. Consider all six legs it leads to the following expression

$$\mathbf{B}\dot{\mathbf{s}} = \mathbf{A}\mathbf{t}_p \tag{11}$$

where $\dot{\mathbf{s}} = \left[\dot{s}_1, ..., \dot{s}_6 \right]^T$ is the 6×1 vector of the actuator speeds, and $\mathbf{A}$ and $\mathbf{B}$ are the 6×6 matrices representing the inverse and forward *Jacobian* of the hexapod and they are defined as

$$\mathbf{A} = \begin{bmatrix} \mathbf{l}_1^T & (\mathbf{R}\bar{\mathbf{p}}_1 \times \mathbf{l}_1)^T \\ \vdots & \vdots \\ \mathbf{l}_6^T & (\mathbf{R}\bar{\mathbf{p}}_6 \times \mathbf{l}_6)^T \end{bmatrix} \tag{12}$$

$$\mathbf{B} = diag\left(\mathbf{u}_1^s \cdot \mathbf{l}_1, ..., \mathbf{u}_6^s \cdot \mathbf{l}_6 \right) \tag{13}$$

Eq.(11) defines the differential relationship between the actuator speeds $\dot{\mathbf{s}}$ and the twist of the moving platform $\mathbf{t}_p$. Rewriting eq.(11) gives

$$\dot{\mathbf{s}} = \mathbf{J}_p \mathbf{t}_p \tag{14}$$

Provided that $\mathbf{B}$ is invertible, the Jacobian matrix of the moving platform $\mathbf{J}_p$ can be given as

$$\mathbf{J}_p = \mathbf{B}^{-1}\mathbf{A} = \left[\mathbf{J}_{p1}^T, ..., \mathbf{J}_{p6}^T \right]^T \tag{15}$$

where

$$\mathbf{J}_{pi} = \left[\frac{\mathbf{l}_i^T}{\mathbf{l}_i^T \mathbf{u}_i^s}, \frac{\left(\mathbf{R}\bar{\mathbf{p}}_i \times \mathbf{l}_i\right)^T}{\mathbf{l}_i^T \mathbf{u}_i^s} \right] \tag{16}$$

for i = 1,..,6. From eq.(14), $\mathbf{t}_p$ can be expressed in terms of $\dot{\mathbf{s}}$ as,

$$\mathbf{t}_p = \mathbf{T}_p \dot{\mathbf{s}} \tag{17}$$

where $\mathbf{T}_p = \mathbf{J}_p^{-1}$.

To obtain the acceleration of the moving platform, taking the time derivative of eq. (14) yields

$$\ddot{\mathbf{s}} = \dot{\mathbf{J}}_p \mathbf{t}_p + \mathbf{J}_p \dot{\mathbf{t}}_p \tag{18}$$

where $\ddot{\mathbf{s}} = \left[\ddot{s}_1, ..., \ddot{s}_6\right]^T$ is the 6×1 vector of the actuator accelerations, $\dot{\mathbf{t}}_p = \left[\mathbf{a}^T, \dot{\boldsymbol{\omega}}^T\right]^T$ is the time derivative of the twist of the moving platform, $\dot{\mathbf{J}}_p$ is the time derivative of the Jacobian matrix of the moving platform obtained by differentiating $\mathbf{J}_p$ with respect to time, that is

$$\dot{\mathbf{J}}_p = \mathbf{B}^{-1}(\dot{\mathbf{A}} - \dot{\mathbf{B}}\mathbf{B}^{-1}\mathbf{A}) \tag{19}$$

where $\dot{\mathbf{A}}$ and $\dot{\mathbf{B}}$ given as

$$\dot{\mathbf{A}} = \begin{bmatrix} (\boldsymbol{\omega}_1 \times \mathbf{l}_1)^T & ((\boldsymbol{\omega} \times \mathbf{R}\bar{\mathbf{p}}_1) \times \mathbf{l}_1 + \mathbf{R}\bar{\mathbf{p}}_1 \times (\boldsymbol{\omega}_1 \times \mathbf{l}_1))^T \\ \vdots & \vdots \\ (\boldsymbol{\omega}_6 \times \mathbf{l}_6)^T & ((\boldsymbol{\omega} \times \mathbf{R}\bar{\mathbf{p}}_6) \times \mathbf{l}_6 + \mathbf{R}\bar{\mathbf{p}}_6 \times (\boldsymbol{\omega}_6 \times \mathbf{l}_6))^T \end{bmatrix} \tag{20}$$

$$\dot{\mathbf{B}} = diag\left(\mathbf{u}_1^s \cdot (\boldsymbol{\omega}_1 \times \mathbf{l}_1), ..., \mathbf{u}_6^s \cdot (\boldsymbol{\omega}_6 \times \mathbf{l}_6)\right) \tag{21}$$

If the mass of the leg is uniformly distributed, then the center of mass is in its middle. The velocity of the center of mass can be given as

$$\dot{\mathbf{c}}_i = \dot{\mathbf{s}}_i + \boldsymbol{\omega}_i \times \frac{\mathbf{l}_i}{2} \tag{22}$$

Upon differentiating eq.(22), the acceleration of the center of mass can be given as

$$\ddot{\mathbf{c}}_i = \ddot{\mathbf{s}}_i + \dot{\boldsymbol{\omega}}_i \times \frac{\mathbf{l}_i}{2} + \boldsymbol{\omega}_i \times (\boldsymbol{\omega}_i \times \frac{\mathbf{l}_i}{2}) \tag{23}$$

To obtain the leg angular velocity and acceleration, denote by $\mathbf{E}_i$ the 3×3 cross-product matrix associated with vector $\mathbf{u}_i^l$, then eq.(9) may be re-written as

$$\mathbf{E}_i \boldsymbol{\omega}_i = \frac{1}{l_i}\left[\mathbf{v} + \boldsymbol{\omega} \times \mathbf{R}\bar{\mathbf{p}}_i - \dot{s}_i \mathbf{u}_i^s\right] \tag{24}$$

Consider all six legs, it forms a set of linear equations containing the unknowns of the leg angular velocity. There are three components of $\boldsymbol{\omega}_i$ for each leg. Because matrix $\mathbf{E}_i$ is a skew symmetric and singular, it is impossible to directly solve eq.(24). However, since the leg does not spin about its longitudinal axis, this indicates (Tsai, 2000)

$$\boldsymbol{\omega}_i \cdot \mathbf{l}_i = 0 \tag{25}$$

In the light of eq.(25), eq. (24) may be rewritten as

$$\mathbf{A}_i \boldsymbol{\omega}_i = \mathbf{e}_i \tag{26}$$

where $\mathbf{A}_i$ is a 4×3 matrix and $\mathbf{e}_i$ is a 4-dimensional vector, and they are defined as

$$\mathbf{A}_i = \begin{bmatrix} \mathbf{E}_i \\ \mathbf{l}_i^T \end{bmatrix} \tag{27}$$

$$\mathbf{e}_i = \frac{1}{l_i} \begin{bmatrix} \mathbf{v} + \boldsymbol{\omega} \times \mathbf{R}\bar{\mathbf{p}}_i - \dot{s}_i \mathbf{u}_i^s \\ 0 \end{bmatrix} \tag{28}$$

Solving eq. (26) leads to the expression for the leg angular velocity

$$\boldsymbol{\omega}_i = \frac{\mathbf{l}_i}{l_i^2} \times \left[\mathbf{v} + \boldsymbol{\omega} \times \mathbf{R}\bar{\mathbf{p}}_i - \dot{s}_i \mathbf{u}_i^s \right] \tag{29}$$

Now eq.(29) is substituted back into eq.(22), and the velocity becomes

$$\dot{\mathbf{c}}_i = \frac{1}{2} \left[\mathbf{v} + \boldsymbol{\omega} \times \mathbf{R}\bar{\mathbf{p}}_i - \dot{s}_i \mathbf{u}_i^s \right] \tag{30}$$

By examining eqs.(29 & 30), it may be noted that the two terms in the brackets are identical. The first term may be expressed as

$$\mathbf{v} + \boldsymbol{\omega} \times \mathbf{R}\bar{\mathbf{p}}_i = [\mathbf{1},\ \mathbf{E}_{pi}]\, \mathbf{t}_p \tag{31}$$

where $\mathbf{E}_{pi}$ is the cross-product matrix of $\mathbf{R}\bar{\mathbf{p}}_i$. In the light of eq.(17), eq.(31) may be related to $\dot{\mathbf{s}}$ as

$$[\mathbf{1},\ \mathbf{E}_{pi}]\, \mathbf{t}_p = \mathbf{T}_{1i} \dot{\mathbf{s}} \tag{32}$$

where $\mathbf{1}$ is the 3×3 identity matrix and $\mathbf{T}_{1i}$ is the 3×6 matrix pertaining to the first term defined as

$$\mathbf{T}_{1i} = [\mathbf{1},\ \mathbf{E}_{pi}]\, \mathbf{T}_p \tag{33}$$

The second term in eqs.(29) and (30) can also be expressed in terms of $\dot{\mathbf{s}}$

$$\dot{s}_i \mathbf{u}_i^s = \mathbf{T}_{2i} \dot{\mathbf{s}} \tag{34}$$

where $\mathbf{T}_{2i}$ is the 3×6 matrix pertaining to the second term defined as

$$\mathbf{T}_{2i} = [\mathbf{0}_3,...,\mathbf{u}_i^s,...,\mathbf{0}_3] \tag{35}$$

In eq.(35), $\mathbf{0}_3$ is the 3-dimensional null vector. The twist of the *i*th leg can be expressed in terms of $\dot{\mathbf{s}}$ as

$$\mathbf{t}_i = \mathbf{T}_i\dot{\mathbf{s}} \tag{36}$$

where $\mathbf{t}_i$ is the twist of the ith leg, i.e. $\mathbf{t}_i = \left[\dot{\mathbf{c}}_i^T, \boldsymbol{\omega}_i^T\right]^T$, and the 6×6 matrix $\mathbf{T}_i$ is given as

$$\mathbf{T}_i = \left[\mathbf{T}_{1i}^T, \mathbf{T}_{2i}^T\right]^T \tag{37}$$

Furthermore, the leg angular acceleration can be obtained by differentiating eq.(26) with respect to time, that is

$$\mathbf{A}_i\dot{\boldsymbol{\omega}}_i = \dot{\mathbf{e}}_i - \dot{\mathbf{A}}_i\boldsymbol{\omega}_i \tag{38}$$

where

$$\dot{\mathbf{A}}_i\boldsymbol{\omega}_i = \begin{bmatrix} (\boldsymbol{\omega}_i \times \mathbf{u}_i^l)\times\boldsymbol{\omega}_i \\ 0 \end{bmatrix} \tag{39}$$

$$\dot{\mathbf{e}}_i = \frac{1}{l_i}\begin{bmatrix} \mathbf{a} + \dot{\boldsymbol{\omega}}\times\mathbf{R}\bar{\mathbf{p}}_i + \boldsymbol{\omega}\times(\boldsymbol{\omega}\times\mathbf{R}\bar{\mathbf{p}}_i) - \ddot{s}_i\mathbf{u}_i^s \\ 0 \end{bmatrix} \tag{40}$$

From eq.(38), vector $\dot{\boldsymbol{\omega}}_i$ representing the angular acceleration of the *i*th leg is given as

$$\dot{\boldsymbol{\omega}}_i = \frac{1}{l_i^2}\left[(\boldsymbol{\omega}_i\times\mathbf{l}_i)\times\left(\mathbf{v}+\boldsymbol{\omega}\times\mathbf{R}\bar{\mathbf{p}}_i - \dot{s}_i\mathbf{u}_i^s\right) + \mathbf{l}_i\times\left(\mathrm{a}+\dot{\boldsymbol{\omega}}\times\mathbf{R}\bar{\mathbf{p}}_i + \boldsymbol{\omega}\times(\boldsymbol{\omega}\times\mathbf{R}\bar{\mathbf{p}}_i) - \ddot{s}_i\mathbf{u}_i^s\right)\right] \tag{41}$$

3. Dynamic modeling

3.1 The natural orthogonal complement method

Prior to performing dynamic modeling of the hexapod, a brief review of the natural orthogonal complement method (Angeles & Lee, 1988) is provided. Consider a system composed of *p* rigid bodies under holonomic constraints, the Newton-Euler equations for each individual body can be written, for *i* = 1,.., *p*, as

$$\mathbf{M}_i\dot{\mathbf{t}}_i = -\mathbf{W}_i\mathbf{M}_i\mathbf{t}_i + \mathbf{w}_i \tag{42}$$

where $\mathbf{t}_i$ is the twist of the *i*th body, $\mathbf{w}_i = \left[\mathbf{n}_i^T, \mathbf{f}_i^T\right]^T$ represent the wrench acting on the *i*th body, $\mathbf{n}_i$ and $\mathbf{f}_i$ are the resultant moment and the resultant force acting at the center of mass. In general $\mathbf{w}_i$ can be decomposed into *working wrench* $\mathbf{w}_i^w$ and *non-working wrench* $\mathbf{w}_i^N$. The former can further be decomposed as

$$\mathbf{w}_i^w = \mathbf{w}_i^a + \mathbf{w}_i^g + \mathbf{w}_i^d \tag{43}$$

where $\mathbf{w}_i^a, \mathbf{w}_i^g$ and $\mathbf{w}_i^d$ are the actuator, gravity and dissipate wrenches, respectively.
In eq. (42), the 6×6 angular velocity matrix $\mathbf{W}_i$ and the 6×6 inertia matrix $\mathbf{M}_i$ are defined as

$$\mathbf{W}_i = \begin{bmatrix} \mathbf{\Omega}_i & \mathbf{O} \\ \mathbf{O} & \mathbf{O} \end{bmatrix}, \ \mathbf{M}_i = \begin{bmatrix} \mathbf{I}_i & \mathbf{O} \\ \mathbf{O} & m_i \mathbf{1} \end{bmatrix} \tag{44}$$

with

$$\mathbf{\Omega}_i = \frac{\partial(\boldsymbol{\omega}_i \times \mathbf{e})}{\partial \mathbf{e}} \tag{45}$$

where $\mathbf{I}_i$ is the 3×3 matrix of the moment of inertia of the ith body, m_i is the body mass, $\mathbf{O}$ denotes the 3×3 null matrix, and $\mathbf{e}$ is an arbitrary vector.
If consider all p bodies, the assembled system dynamics equations are given as

$$\mathbf{M}\dot{\mathbf{t}} = -\mathbf{W}\mathbf{M}\mathbf{t} + \mathbf{w}^W + \mathbf{w}^N \tag{46}$$

where the $6p \times 6p$ generalized mass matrix $\mathbf{M}$ and generalized angular velocity matrix $\mathbf{W}$ are defined as

$$\mathbf{M} \equiv diag(\mathbf{M}_1, \ldots, \mathbf{M}_p), \tag{47}$$

$$\mathbf{W} \equiv diag(\mathbf{W}_1, \ldots, \mathbf{W}_p) \tag{48}$$

and the $6p$-dimensional generalized twist $\mathbf{t}$, generalized working wrench $\mathbf{w}^W$ and generalized non-working wrench $\mathbf{w}^N$ are defined as

$$\mathbf{t} \equiv \begin{bmatrix} \mathbf{t}_1 \\ \vdots \\ \mathbf{t}_p \end{bmatrix}, \ \mathbf{w}^W \equiv \begin{bmatrix} \mathbf{w}_1^W \\ \vdots \\ \mathbf{w}_p^W \end{bmatrix}, \ \mathbf{w}^N \equiv \begin{bmatrix} \mathbf{w}_1^N \\ \vdots \\ \mathbf{w}_p^N \end{bmatrix} \tag{49}$$

It can be shown that the kinematic constraints hold the following relation with the generalized twist

$$\mathbf{K}\mathbf{t} = \mathbf{0}_{6p} \tag{50}$$

where $\mathbf{0}_{6p}$ is the $6p$-dimensional null vector, $\mathbf{K}$ is the $6p \times 6p$ velocity constraint matrix with a rank of m which is equal to the number of independent holonomic constraints. The number of degrees of freedom of the system, i.e. independent variables, is determined as $n = 6p - m$. Denote the independent variables by $\mathbf{s}$, they can be related to the twist as

$$\mathbf{t} = \mathbf{T}\dot{\mathbf{s}} \tag{51}$$

$$\dot{\mathbf{t}} = \mathbf{T}\ddot{\mathbf{s}} + \dot{\mathbf{T}}\dot{\mathbf{s}} \tag{52}$$

where **T** is a $6p \times n$ twist-mapping matrix.

By substituting eq.(51) into eq.(50), the following relation can be obtained

$$\mathbf{K}\mathbf{T} = \mathbf{0}_{6p} \tag{53}$$

where **T** is the natural orthogonal complement of **K**. As shown in (Angeles & Lee, 1988, 1989) the non-working vector $\mathbf{w}^N$ lies in the null space of the transpose of **T**. Thus, if both sides of eq. (46) are multiplied by $\mathbf{T}^T$, in the aid of eqs. (51 & 52), the system dynamics equations can be obtained as

$$\mathbf{I}\ddot{\mathbf{s}} + \mathbf{C}\dot{\mathbf{s}} = \mathbf{T}^T(\mathbf{w}^a + \mathbf{w}^g + \mathbf{w}^d) \tag{54}$$

where the $n \times n$ generalized inertia matrix **I** and coupling matrix **C** are defined as

$$\mathbf{I} \equiv \mathbf{T}^T\mathbf{M}\mathbf{T}\,,\ \mathbf{C} \equiv \mathbf{T}^T(\mathbf{M}\dot{\mathbf{T}} + \mathbf{W}\mathbf{M}\mathbf{T}) \tag{55}$$

Furthermore, by defining the following generalized forces

$$\tau^a = \mathbf{T}^T\mathbf{w}^a, \quad \tau^g = \mathbf{T}^T\mathbf{w}^g, \quad \tau^d = \mathbf{T}^T\mathbf{w}^d, \quad \boldsymbol{\tau}^I = \mathbf{I}\ddot{\mathbf{s}} + \mathbf{C}\dot{\mathbf{s}} \tag{56}$$

the inverse dynamics of the system can be given as

$$\boldsymbol{\tau}^a = \boldsymbol{\tau}^I - \boldsymbol{\tau}^g - \boldsymbol{\tau}^d \tag{57}$$

where $\boldsymbol{\tau}^a$ is the vector representing the applied actuator forces.

3.2 Inverse dynamics

The key in applying the natural orthogonal complement method is to derive the expression for the twist-mapping matrix **T**, which relates the speeds of the independent variables to the generalized twist. For the hexapod under study, the independent variable *s* is the vector representing the actuator displacement, with the total number of six, as defined before. The generalized twist is expressed as

$$\mathbf{t} = \begin{bmatrix} \mathbf{t}_1 \\ \vdots \\ \mathbf{t}_6 \\ \mathbf{t}_{pc} \end{bmatrix} \tag{58}$$

Note that $\mathbf{t}_1$ to $\mathbf{t}_6$ are the twists for the six legs. Since the twist in eq.(36) is defined at the center of mass of the leg, $\mathbf{T}_i$ represents the twist-mapping for the legs. For the moving platform, $\mathbf{t}_{pc}$ is defined as the center of mass which may be expressed as

$$\mathbf{c}_p = \mathbf{h} + \mathbf{R}\bar{\boldsymbol{\rho}} \tag{59}$$

Differentiating eq.(59) gives

$$\dot{\mathbf{c}}_p = \mathbf{v} + \boldsymbol{\omega} \times \mathbf{R}\bar{\boldsymbol{\rho}} \tag{60}$$

In the light of eq.(60), the following relation can be obtained

$$\mathbf{t}_{pc} = \mathbf{H}_p \mathbf{t}_p \tag{61}$$

where $\mathbf{H}_p$ is the 6×6 matrix defined as

$$\mathbf{H}_p = \begin{bmatrix} \mathbf{1} & \mathbf{E}_\rho \\ \mathbf{O} & \mathbf{1} \end{bmatrix} \tag{62}$$

In eq.(62), $\mathbf{E}_\rho$ is the cross-product matrix of $\mathbf{R}\bar{\boldsymbol{\rho}}$. Note that when $\bar{\boldsymbol{\rho}}$ is zero, i.e. the center of mass coincides with the coordinate origin, $\mathbf{H}_p$ becomes an identity matrix, and $\mathbf{t}_{pc} = \mathbf{t}_p$.
The twist-mapping matrix $\mathbf{T}$ for the hexapod under study can be given in the light of eqs.(17), (36) and (62) as

$$\mathbf{T} = \begin{bmatrix} \mathbf{T}_1 \\ \vdots \\ \mathbf{T}_6 \\ \mathbf{H}_p \mathbf{T}_p \end{bmatrix} \tag{63}$$

where $\mathbf{T}$ is a 42×6 matrix. With $\mathbf{T}$, the generalized forces can be defined according to eq.(56), and the applied actuator forces can be determined according to eq.(57).

4. Simulation

4.1 Geometric and inertial parameters

The geometry of the base and the moving platform is shown in Figure 3.

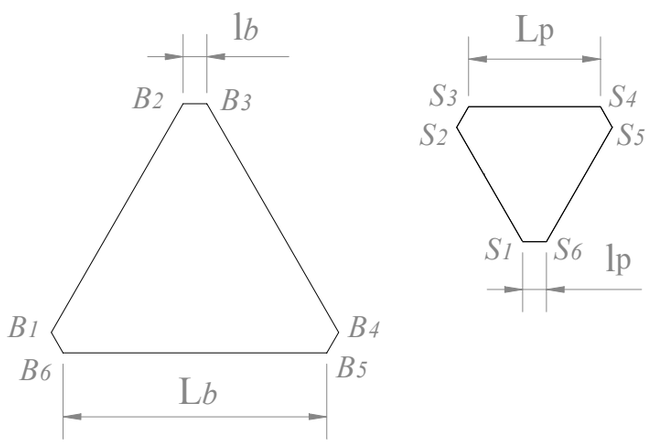

Fig. 3. Geometry of the base and the moving platform

Accordingly, the coordinates of vector $\mathbf{b}_i$ with respect to the fixed frame are given as

$$\mathbf{b}_1 \equiv [L_b/2, -y_b, 0]^T \quad (64a)$$
$$\mathbf{b}_2 \equiv [(L_b + l_b)/2, -l_b c_s, 0]^T \quad (64b)$$
$$\mathbf{b}_3 \equiv [l_b/2, (L_b + l_b)c_s - y_b, 0]^T \quad (64c)$$
$$\mathbf{b}_4 \equiv [-l_b/2, (L_b + l_b)c_s - y_b, 0]^T \quad (64d)$$
$$\mathbf{b}_5 \equiv [(L_b + l_b)/2, l_b c_s - y_b, 0]^T \quad (64e)$$
$$\mathbf{b}_6 \equiv [-L_b/2, -y_b, 0]^T \quad (64f)$$

where L_b and l_b are the long and short side of the base hexagon, $c_s = \cos(30^\circ)$, and $y_b = (L_b/2 + l_b)tg(30^\circ)$. Likewise, the coordinates of vector $\bar{\mathbf{p}}_i$ with respect to the local frame are given as

$$\bar{\mathbf{p}}_1 \equiv [L_p/2, -y_p, 0]^T \quad (65a)$$
$$\bar{\mathbf{p}}_2 \equiv [(L_p + l_p)/2, -l_p c_s, 0]^T \quad (65b)$$
$$\bar{\mathbf{p}}_3 \equiv [l_p/2, (L_p + l_p)c_s - y_p, 0]^T \quad (65c)$$
$$\bar{\mathbf{p}}_4 \equiv [-l_p/2, (L_p + l_p)c_s - y_p, 0]^T \quad (65d)$$
$$\bar{\mathbf{p}}_5 \equiv [(L_p + l_p)/2, l_p c_s - y_p, 0]^T \quad (65e)$$
$$\bar{\mathbf{p}}_6 \equiv [-L_p/2, -y_p, 0]^T \quad (65f)$$

where L_p and l_p are the long and short side of the moving platform hexagon, and $y_p = (L_p/2 + l_p)tg(30^\circ)$. The geometric parameters and inertial parameters are given in Tables 1 and 2, respectively. In Table 1, S is the guideway length, γ is the guideway angle between the guideway and the vertical direction, and l is the length of the leg. These three parameters are the same for all the guideways and legs. Parameters L_b, l_b, L_p and l_p are defined in Figure 3. In Table 2, m is the mass, and I_{xx}, I_{yy} and I_{zz} are the moments of inertia.

S *Guideway length*	γ *Guideway angle*	l *Leg length*	L_b *Long side BP*	l_b *Short side BP*	L_p *Long side MP*	l_p *Short side MP*
0.60 m	45°	0.50 m	1.00 m	0.09 m	0.50 m	0.09m

Table 1. Geometric parameters

	m (kg)	$Ixx = Iyy$ (kg·m2)	Izz (kg·m2)
Platform	3.983	0.068	0.136
Leg	0.398	0.0474	-

Table 2. Inertial parameters

4.2 Numerical example

A simulation program has been developed using Matlab based on the method described in the previous sections. In terms of computation, as can be seen from eq. (54), the inverse dynamics of the hexapods mainly involves the twist-mapping matrix **T** and its derivative, which could be computed numerically for each time interval. This way, it is computationally more efficient. To further speed up computation, parallel computation techniques could be used. As shown in Figure 4, the motion part including actuator speeds and accelerations could be computed in parallel to the inertia part including mass matrix **I** and coupling matrix **C**. Since the program is done in Matlab, parallel computation is not realized. However, this strategy can certinaly be applied to model-based control using the dynamic equations.

In terms of singularity, as can be shown from eq. (63), the twist-mapping matrix **T** becomes degenerate when the moving platform Jacobian $\mathbf{J}_p$ ($\mathbf{T}_p = \mathbf{J}_p^{-1}$) is singular.

The movement of the moving platform is defined in terms of 3-4-5 polynomials that guarantee zero velocities and zero accelerations at the beginning and at the end. The selection of a smooth motion profile is very important for the hexapod as it is operated under high speeds. The conventional machine tools are run at a maximum velocity of 30m/min with a maximum acceleration of 0.3 g. Hexapods can run at a maximum velocity of 100 m/min with a maximum acceleration over 1 g.

The first simulation is for high speed, with a maximum velocity of 102 m/min. The second simulation is for low high speed with a maximum velocity of 30 m/min. In both cases, the hexapod moves a distance of 0.1m along the z axis. The initial position of the moving platform is at $x_o = 0$, $y_o = 0$ and $z_o = 0.7$m. Figure 4 shows the velocity profiles of the moving platform. Figures 5, 6 and 7 show the displacements, velocities and accelerations of the six actuators, respectively. Figure 8 shows the computed actuator forces. The simulations show that high speed motions result in large actuator forces.

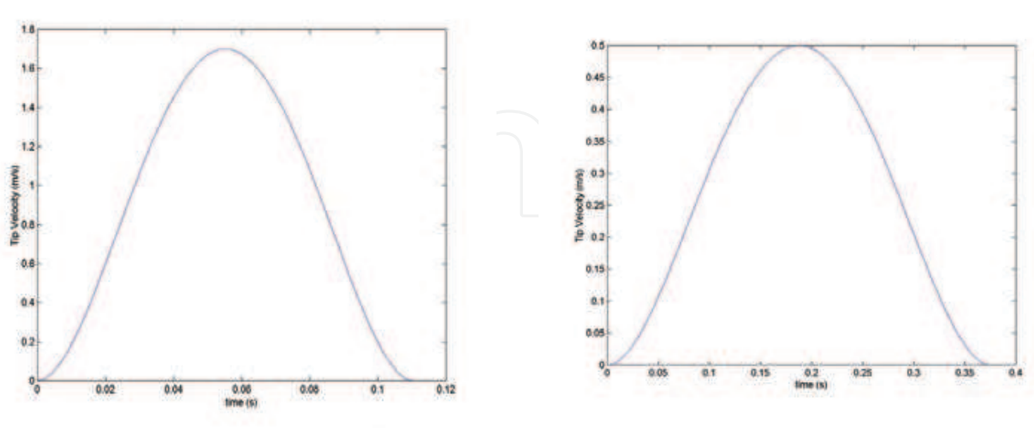

a) High speed (b) Low speed

Fig. 4. Motion Profile of moving platform

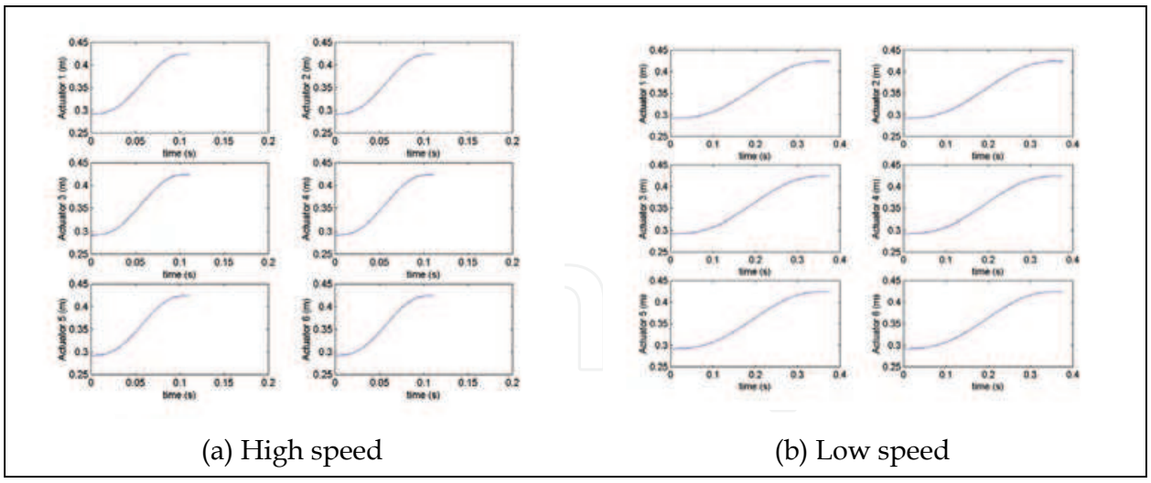

(a) High speed (b) Low speed

Fig. 5. Actuator displacements

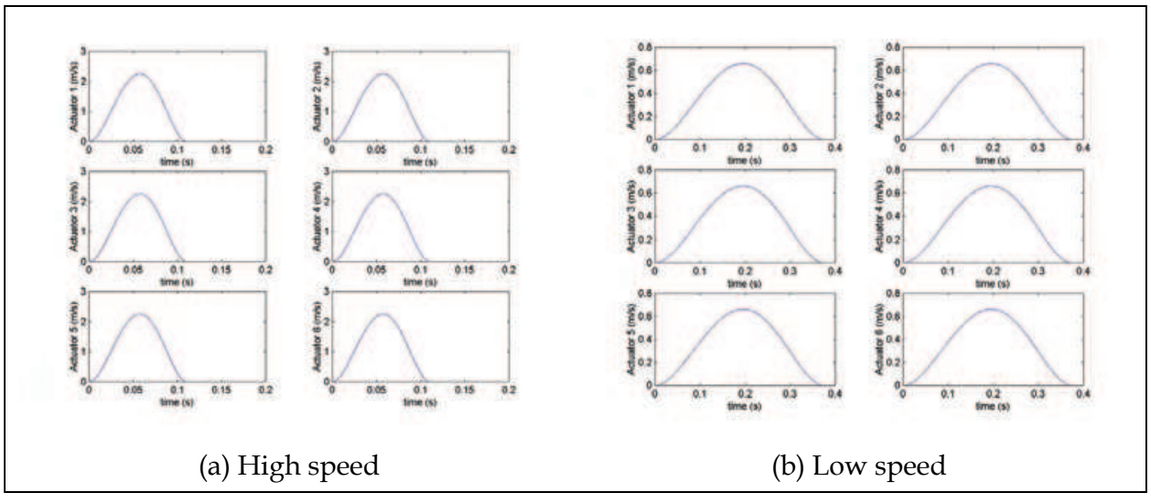

(a) High speed (b) Low speed

Fig. 6. Actuator velocities

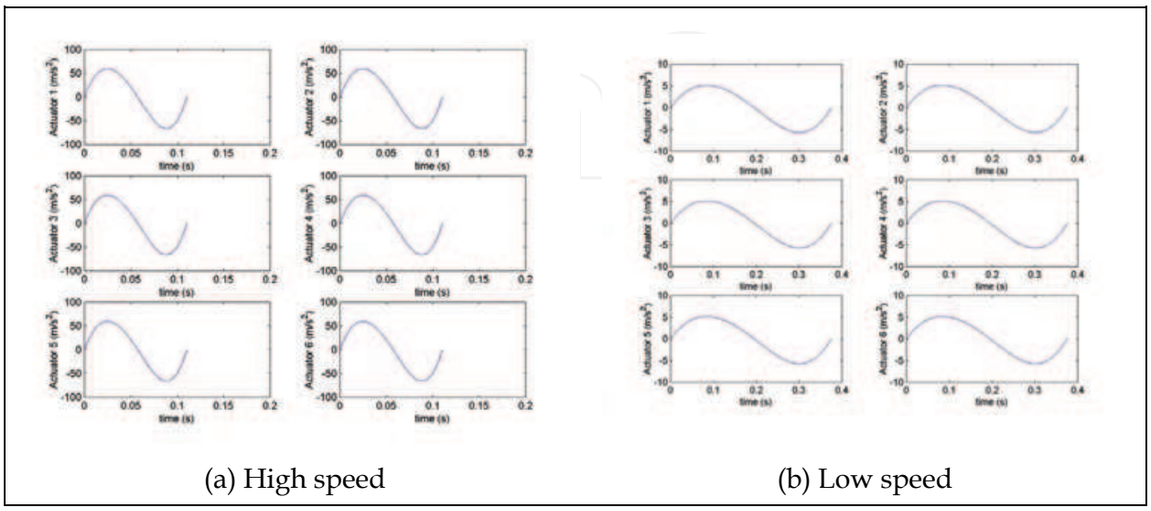

(a) High speed (b) Low speed

Fig. 7. Actuator accelerations

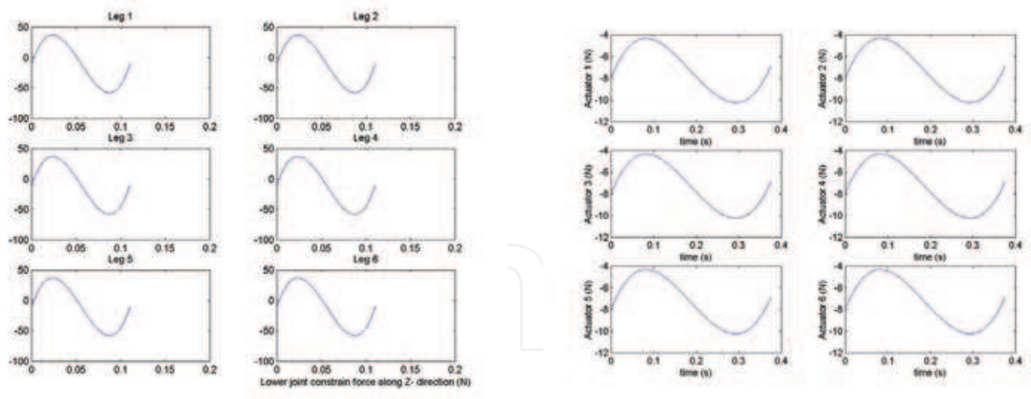

(a) High speed (b) Low speed

Fig. 8. The computed actuator forces

5. Static balancing of the hexapod

The static and dynamic balancing is a classic problem in the theory of machines and mechanisms. In particular, when a mechanism is not statically balanced, the weight of linkage produces force or torque at actuators under static conditions and actuators have to contribute to support the weight of the moving links for any configurations. The problem becomes more serious for the parallel manipulator applied as flight simulator where the weight of the moving platform is very large with respect to the masses of the links. Static balancing also called *gravity compensation* is important. If the forces/toques exerted by joint actuators are reduced, the full potential of machine will be improved.
In this paragraph, following the same approach presented by Gosselin, the static balancing of the hexapod with the fixed-length legs is studied.

5.1 Static balancing using counterweight

The static balancing of the parallel manipulator under study is investigated using counterweights. The base coordinate frame Oxyz frame, is fixed to the base with Z-axis pointing vertically upward and the moving coordinate frame O'x'y'z' is attached to the moving platform. The Cartesian coordinates used to describe the pose of the platform are as shown in Fig. 9 given by the position of O' with respect to the fixed frame and the orientation of the platform represented by the rotation matrix $\mathbf{Q}$

$$\mathbf{Q} = \begin{bmatrix} q_{11} & q_{12} & q_{13} \\ q_{21} & q_{22} & q_{23} \\ q_{31} & q_{32} & q_{33} \end{bmatrix} \tag{66}$$

Using the counterweights, static balancing is obtained if the global center mass of the mechanism is kept stationary at any values of the independent variables. To choose an suitable constant, namely

$$M\mathbf{r} = \mathbf{0} \tag{67}$$

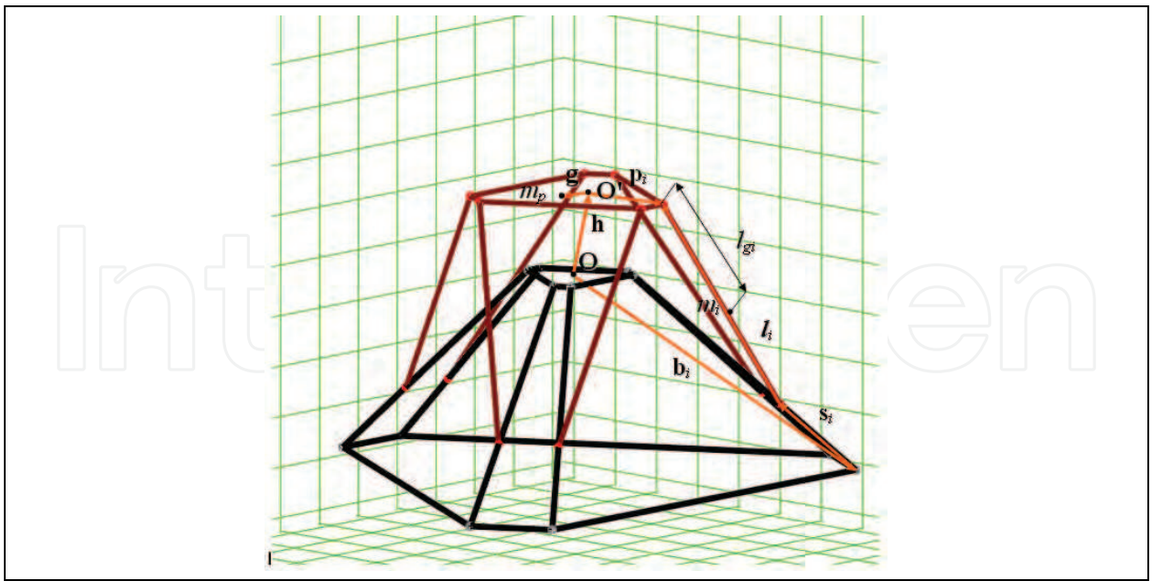

Fig.9 Kinematic mode

where **r** is the position vector of the global mass center, and M is:

$$M = m_p + \sum_{i=1}^{6} m_i \tag{68}$$

where m_p is the mass of the platform, m_i is the mass of the leg. The global centre of the mass of the manipulator is written as

$$M\mathbf{r} = m_p\mathbf{r}_p + \sum_{i=1}^{6} m_i\mathbf{r}_i \tag{69}$$

where $\mathbf{r}_p$ is the platform center of the mass, $\mathbf{r}_i$ is the leg center of the mass. From Fig. 9, vectors $\mathbf{r}_p$, $\mathbf{r}_i$ can be derived, and substituted into eq.(69), yielding

$$M\mathbf{r} = m_p\left(\mathbf{h} + \mathbf{Q}\cdot\mathbf{g}\right) + \sum_{i=1}^{6} m_i\left[\left(\mathbf{h} + \mathbf{Q}\cdot\mathbf{p}_i\right) - \left(\mathbf{h} + \mathbf{Q}\cdot\mathbf{p}_i - \mathbf{b}_i - \mathbf{s}_i\right)\frac{l_{gi}}{l_i}\right] \tag{70}$$

where **g** is the vector center of mass of the moving platform with respect to the frame O'x'y'z', **h** is the position of O' with respect to the fixed frame, $\mathbf{p}_i$ is the position of the spherical joint with respect to the moving coordinate frame, $\mathbf{b}_i$ is the position of the lower end of the guideway with respect to the fixed frame, $\mathbf{l}_i$ is the length of the leg, $\mathbf{s}_i$ can be written, for i=1,…,6, as

$$\mathbf{s}_i = \rho_i \cdot \hat{\mathbf{s}}_i \tag{71}$$

where $\hat{\mathbf{s}}_i$ is the unit vector of guideway, ρ_i is the independent variable of the prismatic joint. In concise form, eq. (70) is expressed as

$$M\boldsymbol{r} = A_1\mathbf{h} + \mathbf{QB} + \sum_{i=1}^{6} A_{5i}\mathbf{s}_i + \mathbf{A}_0 \tag{72}$$

where

$$A_1 = m_p + \sum_{i=1}^{6} m_i\left(1 - \frac{l_{gi}}{l_i}\right) \tag{73}$$

$$\mathbf{B} = m_p\mathbf{g} + \sum_{i=1}^{6} m_i\mathbf{p}_i\left(1 - \frac{l_{gi}}{l_i}\right) \tag{74}$$

$$A_{5i} = m_i\frac{l_{gi}}{l_i} \quad \text{, for } i\text{=1,..,6} \tag{75}$$

$$\mathbf{A_0} = \sum_{i=1}^{6} A_{5i}\mathbf{b}_i \tag{76}$$

The conditions for static balancing can be given for i=1,..,6, as follows:

$$A_1 = 0,\ \mathbf{B} = 0,\ A_{5i} = 0,\ \mathbf{A}_0 = 0 \tag{77}$$

From conditions $A_{5i} = 0$, i=1,..,6, one can obtain

$$l_{gi} = 0 \tag{78}$$

By condition $A_1 = 0$, one can obtain

$$m_p = -\sum_{i=1}^{6} m_i \tag{79}$$

Eq.(79) shows that the balancing by counterweight is impossible. If it was substituted in the condition B= 0,

$$m_p\,\mathbf{g} + \sum_{i=1}^{6} m_i\,\mathbf{p}_i = \mathbf{0} \tag{80}$$

then one can obtain

$$\mathbf{g} = \frac{\sum_{i=1}^{6} m_i\mathbf{p}_i}{\sum_{i=1}^{6} m_i} \tag{81}$$

From eq. (81), it shows that the manipulator could be balanced by a device that provide a force that is

1. equal to the weight of the links and the platform;
2. in opposite direction of the weight.

5.2 Static balancing wit a pantograph counterweight

Since it is shown that the static balancing of the examined mechanism is impossible with the help of counterweights, we propose a method to add a pantograph connecting the moving platform O' to the fixed platform O, as shown in Fig. 10. The pantograph is a device that allows to keep two end points on the same line and keep their distance at the centre with a constant ratio. In this application it is possible to use a pantographs with two or more mesh as shown in Fig. 10 and Fig. 11, respectively. In both case the manipulator is balanced. The pantograph is fixed to the moving platform on the point O' by a spherical joint and fixed to the point O by an universal joint. The leg counterweight is shown in Fig.12.

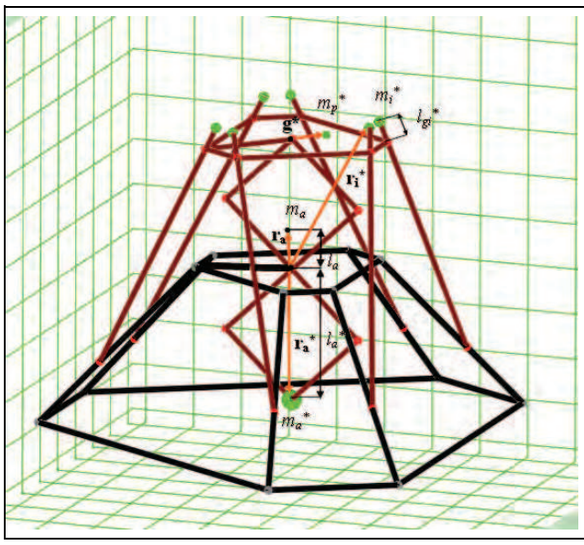

Fig. 10. Model with counterweights mass

Fig. 11. Balanced Hexapod using pantograph

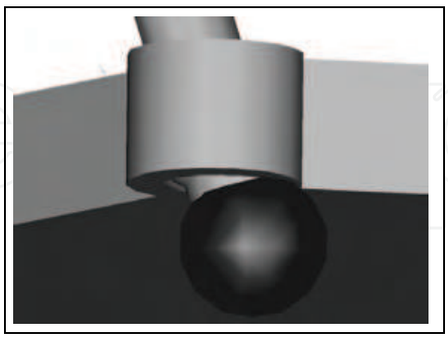

Fig. 12. Leg counterweight

In this case, the mass M becomes,

$$M = m_p + m_p^* + m_a + m_a^* + \sum_{i=1}^{6} m_i + \sum_{i=1}^{6} m_i^* \tag{82}$$

where m_p and m_p^* are the mass of the platform and the mass of the platform counterweight, m_i and m_i^* are the mass of the legs and the mass of the legs counterweights, m_a and m_a^* are the mass of the pantograph and the mass of the of the pantograph counterweight. In this case, the global center of the mass of the manipulator is written as

$$M\mathbf{r} = m_p\mathbf{r}_p + m_p^*\mathbf{r}_p^* + m_a\mathbf{r}_a + m_a^*\mathbf{r}_a^* + \sum_{i=1}^{6} m_i\mathbf{r}_i + \sum_{i=1}^{6} m_i^*\mathbf{r}_i^* \tag{83}$$

where $\mathbf{r}_p$ and $\mathbf{r}_p^*$ are the platform center of the mass and the platform counterweight position, $\mathbf{r}_i$ and $\mathbf{r}_i^*$ are the legs center of the mass and the legs counterweight position, $\mathbf{r}_a$ and $\mathbf{r}_a^*$ are the pantograph center of the mass and the pantograph counterweight position. From Figs. 9-10, vectors $\mathbf{r}_p$, $\mathbf{r}_p^*$, $\mathbf{r}_a$, $\mathbf{r}_a^*$, $\mathbf{r}_i$ and $\mathbf{r}_i^*$ can be derived and substituted into eq.(83), yielding

$$\begin{aligned} M\mathbf{r} &= m_p\left(\mathbf{h}+\mathbf{Q}\cdot\mathbf{g}\right) + m_p^*(\mathbf{h}+\mathbf{Q}\cdot\mathbf{g}^*) + m_a\left(\mathbf{h}\frac{l_a}{|\mathbf{h}|}\right) + m_a^*\left(\mathbf{h}\frac{l_a^*}{|\mathbf{h}|}\right) + \\ &+\sum_{i=1}^{6} m_i\left[\left(\mathbf{h}+\mathbf{Q}\cdot\mathbf{p}_i\right) - \left(\mathbf{h}+\mathbf{Q}\cdot\mathbf{p}_i-\mathbf{b}_i-\mathbf{s}_i\right)\frac{l_{gi}}{l_i}\right] + \\ &+\sum_{i=1}^{6} m_i^*\left[\left(\mathbf{h}+\mathbf{Q}\cdot\mathbf{p}_i\right) - \left(\mathbf{h}+\mathbf{Q}\cdot\mathbf{p}_i-\mathbf{b}_i-\mathbf{s}_i\right)\frac{l_{gi}^*}{l_i}\right] \end{aligned} \tag{84}$$

where, l_a is the center of mass of the pantograph with respect to the fixed frame, l_a^* is the pantograph counterweight position with respect to the fixed frame, l_{gi} is the length of the leg counterweight link, l_i is the length of the leg, $\mathbf{s}_i$ can be written, for i=1,...,6, as

$$\mathbf{s}_i = \rho_i \cdot \hat{\mathbf{s}}_i \tag{85}$$

In concise form, eq.(84) can be expressed as

$$M\boldsymbol{r} = A_1\mathbf{h} + \mathbf{QB} + \sum_{i=1}^{6} A_{5i}\mathbf{s}_i + \mathbf{A}_0 \tag{86}$$

where

$$A_1 = m_p + m_p^* + m_a\frac{l_a}{|\mathbf{h}|} + m_a^*\frac{l_a^*}{|\mathbf{h}|} + \sum_{i=1}^{6} m_i\left(1-\frac{l_{gi}}{l_i}\right) + \sum_{i=1}^{6} m_i^*\left(1-\frac{l_{gi}^*}{l_i}\right) \tag{87}$$

$$\mathbf{B} = m_p\mathbf{g} + m_p^*\mathbf{g}^* + \sum_{i=1}^{6} m_i\mathbf{p}_i\left(1-\frac{l_{gi}}{l_i}\right) + \sum_{i=1}^{6} m_i^*\mathbf{p}_i\left(1-\frac{l_{gi}^*}{l_i}\right) \tag{88}$$

$$A_{5i} = m_i\frac{l_{gi}}{l_i} + m_i^*\frac{l_{gi}^*}{l_i}\ ,\ i=1,..,6 \tag{89}$$

$$\mathbf{A_0} = \sum_{i=1}^{6} A_{5i}\mathbf{b}_i \tag{90}$$

The conditions for static balancing can be given, for i =1,..,6, as follows

$$A_1 = 0,\ \mathbf{B} = 0,\ A_{5i} = 0,\ \mathbf{A}_0 = 0 \tag{91}$$

From conditions $A_{5i} = 0$, for i=1,..,6, one can obtain

$$m_i \frac{l_{gi}}{l_i} + m_i^* \frac{l_{gi}^*}{l_i} = 0 \tag{92}$$

From eq. (92), for i=1,..,6, the following is obtained

$$l_{gi}^* = -\frac{m_i\, l_{gi}}{m_i^*} \tag{93}$$

By condition $A_1 = 0$, i.e.,

$$m_p + m_p^* + \sum_{i=1}^{6}(m_i + m_i^*) + m_a \frac{l_a}{|\mathbf{h}|} + m_a^* \frac{l_a^*}{|\mathbf{h}|} = 0 \tag{94}$$

one can obtain

$$l_a^* = -\frac{|\mathbf{h}|}{m_a^*}\left(m_p + m_p^* + \sum_{i=1}^{6}\left(m_i + m_i^*\right) + m_a \frac{l_a}{|\mathbf{h}|}\right) \tag{95}$$

Finally, condition **B**= 0 leads to the following

$$m_p\,\mathbf{g} + m_p^*\,\mathbf{g}^* + \sum_{i=1}^{6}\left(m_i + m_i^*\right)\mathbf{p}_i = \mathbf{0} \tag{96}$$

Eq.(96) shows that the static balancing can be achieved by fixing the global center of the mass of the moving platform, that of the legs and their counterweights at the same position, O'. In order to obtain it, the platform counterweight should be placed in the position:

$$\mathbf{g}^* = \frac{m_p\,\mathbf{g} + \sum_{i=1}^{6}\left(m_i + m_i^*\right)\mathbf{p}_i}{m_p^*} \tag{97}$$

Simulation is carried out to demonstrate the proposed method. The results are shown in Figs. 13-14, from which it can be seen that the centre of mass of the robot is non-stationary for non balanced case, while it is fixed for the balanced case.
After static balancing the global mass of the device increases by

$$\Delta M = m_p^* + m_a + m_a^* + \sum_{i=1}^{6} m_i^* \tag{98}$$

The negative effect for the dynamic performance by the increasing global mass can be reduced by optimum design of the pantograph. A graph can be arranged to provide such help. Fig. 15 shows the ratios,

$$\frac{M+\Delta M}{M}, \frac{I_i + I_i^*}{I_i}, \frac{I_a + I_a^*}{I_a}, \tag{99}$$

which vary respect to the ratio r_a^*/h and l_{gi}^*/l_{gi} and where I_i is the moment of inertia of the leg, I_i^* is the moment of inertia of the leg counterweight whit respect of $\mathbf{P}_i$, I_a is the moment of inertia of the moving platform and I_a^* is the moment of inertia of the pantograph counterweight with respect of O. It should be noted that with a suitable design it is possible to reduce ΔM at the same time, it may increase I_i and I_a. The effect of gravity compensation on the dynamic performances was studied in detail in (Xi, 1999).

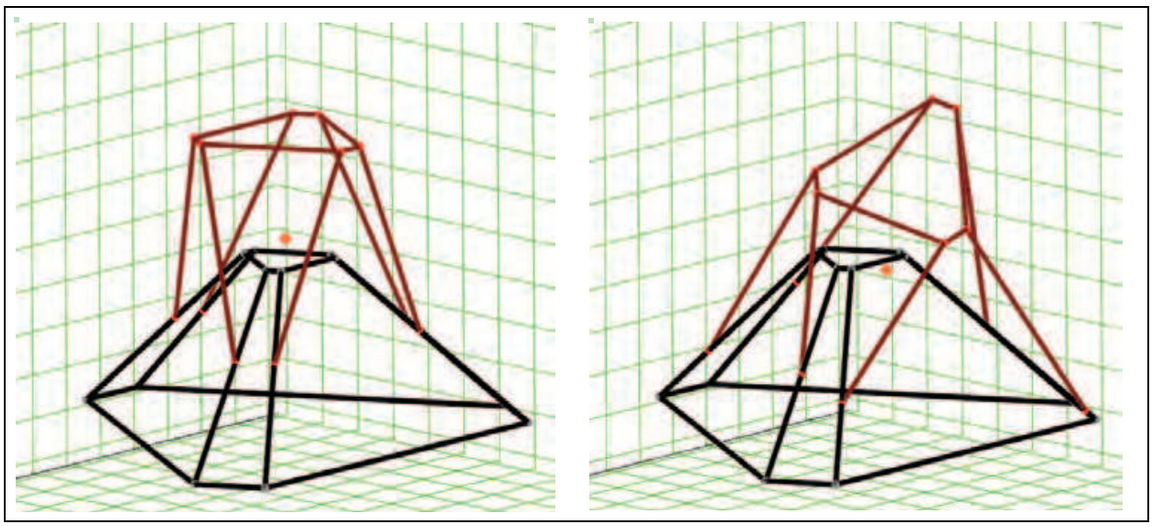

Fig. 13. Mobile center of mass Hexapod

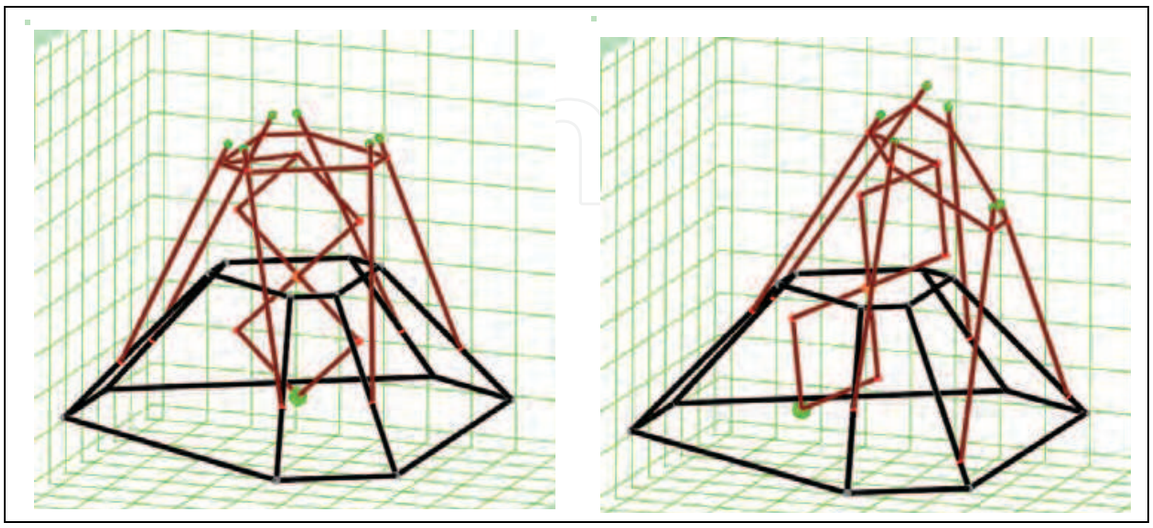

Fig. 14. Fixed center of mass of Balanced Hexapod

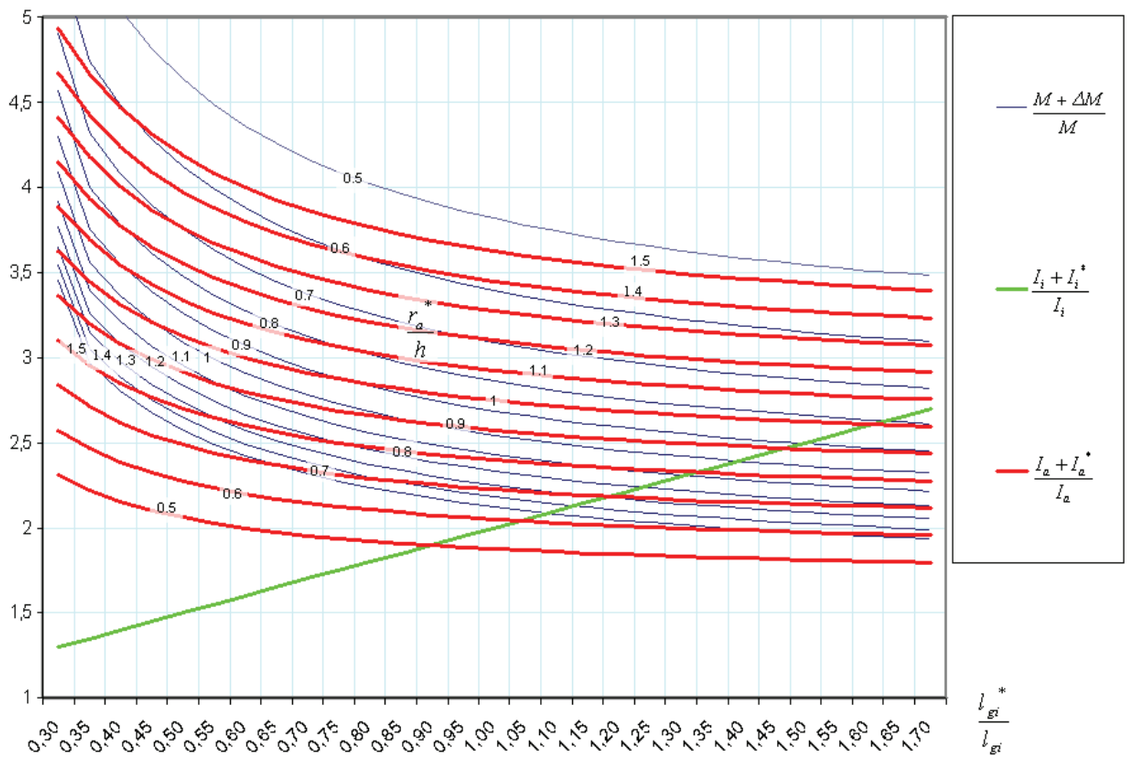

Figure 15. Graph for optimum design

	Input	
Mobile platform		
mass [kg]	short side [mm]	long side [mm]
8	200	800
Fixed platform 1		
mass [kg]	short side [mm]	long side [mm]
/	100	400
Fixed platform 2		
mass [kg]	short side [mm]	long side [mm]
/	250	1000
leg		
mass [kg]	l_i [mm]	l_{gi} [mm]
0.5	750	375
Pantograph		
mass [kg]	side length [mm]	$\mathbf{r_a}$ [mm]
3	100	0
	Output	
m_a^* [kg]	m_i^* [kg]	
17	1	

Table 3. Geometric and inertial parameters

7. Conclusion

In this chapter, the inverse dynamics of hexapods with fixed-length legs is analyzed using the natural orthogonal complement method, with considering the mass of the moving platform and those of the legs. A complete kinematics model is developed, which leads to an explicit expression for the twist-mapping matrix. Based on that, the inverse dynamics equations are derived that can be used to compute the required applied actuator forces for the given movement of the moving platform. The developed method has been implemented and demonstrated by simulation.

Successively, the static balancing of hexapods is addressed. The expression of the global center of mass is derived, based on which a set of static balancing equations has been obtained. It is shown that this type of parallel mechanism cannot be statically balanced by counterweights because prismatic joints do not have a fixed point to pivot as revolute joints. A new design is proposed to connect the centre of the moving platform to that of the fixed platform by a pantograph. The conditions for static balancing are derived. This mechanism is able to release the actuated joints from the weight of the moving legs for any configurations of the robot.

In the future research the leg inertia will be include for modeling the dynamics of the hexapod for high-speed applications.

8. References

Angeles, J. & Lee, S. (1988). The Formulation of Dynamical Equations of Holonomic Mechanical Systems Using a Natural Orthogonal Complement, *ASME J. Applied Mechanics*, Vol. 55, pp. 243-244, ISSN: 0021-8936

Angeles, J. & Lee, S. (1989). The Modeling of Holonomic Mechanical Systems Using a Natural Orthogonal Complement, *Trans. Canadian Society of Mechanical Engineering*, Vol. 13, No. 4, pp. 81-89, ISSN: 0315-8977

Angeles, J. & Ma, O. (1988). Dynamic Simulation of n-axis Serial Robotic Manipulators Using a Natural Orthogonal Complement, *The International Journal of Robotics Research*, Vol. 7, No. 5, pp. 32-47, ISSN: 0278-3649

Do, W. Q. D. & Yang, D. C. H. (1988). Inverse Dynamics and Simulation of a Platform Type of Robot, *The International Journal of Robotics Research*, Vol. 5, No. 3, pp. 209-227, ISSN: 0278-3649

Fichter, E. F. (1986). A Stewart Platform-based Manipulator: General Theory and Practical Construction, *The International Journal of Robotics Research*, Vol. 5, No. 2, pp. 157-182, ISSN: 0278-3649

Fijany, A., & Bejezy, A. K., (1991). Parallel Computation of Manipulator Inverse Dynamics, *Journal of Robotic Systems*, Vol. 8, No. 5, pp. 599-635, ISSN: 0741-2223

Geng, Z.; Haynes, L. S.; Lee, T. D. & Carroll, R. L. (1992). On the Dynamic and Kinematic Analysis of a Class of Stewart Platforms, *Robotics and Autonomous Systems*, Vol. 9, No. 4, pp. 237-254, ISSN: 0921-8890

Gosselin, C. M. & Wang, J. (1998). On the design of gravity-compensated six-degree-of-freedom parallel mechanisms, *Proceedings of IEEE International Conference on Robotics and Automation*, Leuven, Belgium, May 1998, ISBN: 0-7803-4300-X

Hashimoto, K. and Kimura, H., (1989). A New Parallel Algorithm for Inverse Dynamics, *The International Journal of Robotics Research*, Vol. 8, No. 1, pp. 63-76, ISSN: 0278-3649

Hervé, J. M. (1986). Device for counter-balancing the forces due to gravity in a robot arm, *United States Patent,* 4,620,829

Honegger, M.; Codourey, A. & Burdet, E. (1997). Adaptive Control of the Hexaglide a 6 DOF Parallel Manipulator, *Proceedings of the IEEE International Conference on Robotics and Automation,* Albuquerque, NM, April 1997, ISBN: 0-7803-3612-7

Kazerooni, H. & Kim, S. (1990). A new architecture for direct drive robot, Proceedings of the ASME Mechanism Conference, Vol.DE-25, pp. 21-28, Sept. 16-19, 1990, Chicago, IL

Nathan, R. H., (1985). A constant force generation mechanism, *ASME Journal of Mechanism, Transmissions, and Automation in Design*, Vol. 107, No. 4, pp 508-512, ISSN: 0738-0666

Pritschow, G., & Wurst, K.–H., (1997). Systematic Design of Hexapods and Other Parallel Link Systems, *Annals of the CIRP*, Vol. 46/1, pp. 291-295, Elsevier, ISSN: 0007-8506

Saha, K.S. & Angeles, J. (1991). Dynamics of Nonholonomic Mechanical Systems Using a Natural Orthogonal Complement, *ASME Journal of Applied Mechanics*, Vol. 58, pp.238-243, ISSN: 0021-8936

Streit, D.A. & Gilmore, B.J. (1989). Perfect spring equilibrator for rotatable bodies, *ASME Journal of Mechanisms, Transmissions, and Automation in Design*, Vol. 111, No. 4, pp. 451-458, ISSN: 0738-0666

Streit, D.A. & Shin, E. (1990). Equilibrators for planar linkage. *Proceedings of the ASME Mechanism Conference*, Vol. DE-25, pp. 21-28, Cincinnati, OH, , May 1990, Chicago, ISBN: 0-8186-9061-5

Sugimoto, K. (1987). Kinematic and Dynamic Analysis of Parallel Manipulators by Means of Motor Algebra, *ASME Journal Mechanisms, Transmissions, and Automation in Design*, Vol. 109, pp. 3-7, ISSN: 0738-0666

Susuki, M.; Watanabe K.; Shibukawa, T.; Tooyama, T. & Hattori, K. (1997). Development of Milling Machine with Parallel Mechanism, *Toyota Technical Review*, Vol. 47, No. 1, pp. 125-130

Tlusty, J.; Ziegert, J. & Ridgeway, S. (1999). Fundamental Comparison of the Use of Serial and Parallel Kinematics for Machine Tools, *Annals of the CIRP*, Vol. 48, pp. 351-356, Elsevier, ISSN: 0007-8506

Tsai, L. W. (2000). Solving the Inverse Dynamics of a Stewart-Gough Manipulator by the Principle of Virtual Work, *ASME Journal of Mechanical Design*, Vol. 122, pp. 3-9, ISSN: 1050-0472

Ulrich, N. & Kumar, V. (1991). Passive mechanical gravity compensation for robot manipulators, Proceedings of the IEEE International Conference on Robotics and *Automation*, pp. 1536-1541, Sacramento, CA, USA, April 1991, ISBN: 0-8186-2163-X

Walsh, G.J.; Strei, D.A & Gilmore, B.J. (1991). Spatial spring equilibrator theory, *Mechanism and Machine Theory*, Vol. 26, No 2, pp. 155-170, ISSN: 0094-114X

Wang, J. & Gosselin, C. M. (2000). Static balancing of spatial four-degree-of freedom parallel mechanisms, *Mechanism and Machine Theory*, Vol. 35, pp. 563-592, ISSN: 0094-114X

Wang, J. & Gosselin, C.M. (1999). Static balancing of spatial three degree freedom parallel mechanism, *Mechanism and Machine Theory*, Vol. 34, pp. 437-452, ISSN 0094-114X

Xi F.; Russo, A. & Sinatra, R., (2005). Static Balancing of parallel robots, *Mechanism and Machine Theory*, Vol. 40, No 2, pp. 131-258, ISSN: 0094-114X

Xi, F. & Sinatra, R. (1997). Effect of Dynamic Balancing on Four-bar Linkage Vibrations, *Mechanism and Machine Theory*, Vol. 32, No. 6, pp.715-728, ISSN: 0094-114X

Xi, F. & Sinatra, R. (2002). Inverse Dynamics of Hexapods using the Natural Orthogonal Complement Methods, *Journal of Manufacturing Systems*, Vol. 21, No 2, pp.73-82, ISSN: 0258-6125

Xi, F. (1999). Dynamic Balancing of Hexapods for High-speed Applications, *Robotica*, Vol. 17, pp. 335-342, ISSN: 0263-5747

Zanganesh, K. E.; Sinatra, R. & Angeles J. (1997). Dynamics of a Six-Degree-of-Freedom Parallel Manipulator with Revolute Legs, *Robotica,* Vol. 15, pp. 385-394, ISSN: 0263-5747.

Parallel Manipulators, towards New Applications

Edited by Huapeng Wu

ISBN 978-3-902613-40-0
Hard cover, 506 pages
Publisher I-Tech Education and Publishing
Published online 01, April, 2008
Published in print edition April, 2008

In recent years, parallel kinematics mechanisms have attracted a lot of attention from the academic and industrial communities due to potential applications not only as robot manipulators but also as machine tools. Generally, the criteria used to compare the performance of traditional serial robots and parallel robots are the workspace, the ratio between the payload and the robot mass, accuracy, and dynamic behaviour. In addition to the reduced coupling effect between joints, parallel robots bring the benefits of much higher payload-robot mass ratios, superior accuracy and greater stiffness; qualities which lead to better dynamic performance. The main drawback with parallel robots is the relatively small workspace. A great deal of research on parallel robots has been carried out worldwide, and a large number of parallel mechanism systems have been built for various applications, such as remote handling, machine tools, medical robots, simulators, micro-robots, and humanoid robots. This book opens a window to exceptional research and development work on parallel mechanisms contributed by authors from around the world. Through this window the reader can get a good view of current parallel robot research and applications.

INTECH
open science | open minds

InTech Europe
University Campus STeP Ri
Slavka Krautzeka 83/A
51000 Rijeka, Croatia
Phone: +385 (51) 770 447
Fax: +385 (51) 686 166
www.intechopen.com

InTech China
Unit 405, Office Block, Hotel Equatorial Shanghai
No.65, Yan An Road (West), Shanghai, 200040, China
中国上海市延安西路65号上海国际贵都大饭店办公楼405单元
Phone: +86-21-62489820
Fax: +86-21-62489821

IntechOpen